Yuzuncu Yil University
Journal of the Institute of Natural & Applied Sciences

https://dergipark.org.tr/en/pub/yyufbed

Research Article

Green Synthesis and Characterization of Fe_2O_3 Nanoparticles

Başak DOĞRU MERT

Adana Alparslan Türkeş Science and Technology University, Faculty of Engineering, Department of Energy Systems Engineering, 01250, Adana, Türkiye
Başak DOĞRU MERT, ORCID No: 0000-0002-2270-9032
Corresponding author e-mail: bdogrumert@atu.edu.tr

Article Info

Received: 03.04.2023
Accepted: 22.08.2023
Online December 2023

DOI:10.53433/yyufbed.1276192

Keywords
Green synthesis,
Iron (III) oxide,
Nanoparticle

Abstract: The aim of this study is to produce iron III oxide (Fe_2O_3) nanoparticles due to their wide application area. The ethanolic extract of curcuma was used in the synthesis method due to number of advantages. These benefits include being inexpensive, widely accessible, simple to extract, and less prone to contamination. The produced particles were analyzed via scanning electron microscope (SEM), energy dispersive analysis (EDX), and transmission electron microscope (TEM). Furthermore, the zeta potential of Fe_2O_3 particles was determined, ultraviolet–visible spectroscopy (UV) analysis and fourier transform infrared spectroscopy (FTIR) analysis were done. According to the results obtained, granular nanoparticles with particle sizes ranging from 30 to 80 nm were synthesized and it was determined that they were sufficiently stable.

Fe_2O_3 Nanoparçacıkların Yeşil Sentezi ve Karakterizasyonu

Makale Bilgileri

Geliş: 03.04.2023
Kabul: 22.08.2023
Online Aralık 2023

DOI:10.53433/yyufbed.1276192

Anahtar Kelimeler
Demir (III) oksit,
Nanopartikül,
Yeşil sentez

Öz: Bu çalışmanın amacı geniş uygulama alanları nedeniyle demir III oksit (Fe_2O_3) nanoparçacıkları üretmektir. Birçok avantajı nedeniyle sentez yönteminde zerdeçalın etanolik ekstraktı kullanılmıştır. Bu avantajlar arasında ucuz olması, yaygın olarak erişilebilir olması, ekstaksiyonlarının basit olması ve kontaminasyona daha az eğilimli olması yer alır. Üretilen parçacıklar, taramalı elektron mikroskobu (SEM), enerji dağılımlı X-Ray analizi (EDX) ve geçirimli elektron mikroskobu (TEM) ile analiz edildi. Ayrıca Fe_2O_3 partiküllerinin zeta potansiyeli belirlendi, ultraviyole-görünür bölge spektroskopisi (UV) analizi ve fourier dönüşümlü kızılötesi spektroskopisi (FTIR) analizi yapıldı. Elde edilen sonuçlara göre tanecik boyutu 30 ile 80 nm arasında değişen granüler şekilli nanopartiküller sentezlendi ve yeterince kararlı oldukları tespit edildi.

1. Introduction

The synthesis of metal nanoparticles is an important topic of research because to the unique features those nanoparticles have in comparison to their bulk counterparts. Metal nanoparticles are essential for various reasons, including size-dependent features such as; metal nanoparticles display unique size-dependent properties that are not observed in bulk materials (Sarkar et al., 2017). For example, as the size of a nanoparticle decreases, its surface area-to-volume ratio increases, which can enhance its reactivity and catalytic activity (Lassoued et al., 2017). The properties of metal nanoparticles can be tuned by controlling their size, shape, and surface chemistry (Ali et al., 2017). This makes them exceedingly adaptive and useful for a wide range of applications, from electronics to catalysis (Lassoued et al., 2017). Nanoparticles, for example, can be very effective catalysts for chemical reactions or effective sensors for detecting pollutants (Janusz et al., 1999). Metal

nanoparticle use is expanding quickly into new fields, such as nanomedicine, where it is being investigated for uses in medication delivery and imaging (Selvaraj et al., 2022). In general, metal nanoparticle production is critical for improving our comprehension of their special features and for creating new applications that can take advantage of these properties. There are several techniques for the synthesis of metal nanoparticles such as chemical reduction; physical methods; electrochemical methods; microemulsion; green synthesis, etc (Mohammadi et al., 2012; Ali et al., 2017; Rydz et al., 2019; Wei et al., 2023).

Chemical reduction is the process of reducing metal salts in a solution to generate nanoparticles. The reduction is commonly accomplished by adding a reducing agent to the metal salt solution, such as sodium borohydride or hydrazine (Wei et al., 2023). The size and shape of the nanoparticles can be controlled by adjusting the concentration of the reactants and the reaction conditions (Lassoued et al., 2017). Metal nanoparticles can be produced using physical techniques such as laser ablation, arc discharge, and sputtering. A high-powered laser is used in laser ablation to evaporate a metal target, which then condenses into nanoparticles. An electric arc is employed in arc discharge to vaporize a metal target, which then condenses into nanoparticles. Metal ions are reduced on an electrode to generate nanoparticles using electrochemical techniques. By altering the electrode potential and the reaction conditions, the size and form of the nanoparticles may be adjusted (Rizvi et al., 2022). Surfactants and co-surfactants are used in micro emulsion to stabilize metal ions in a solution and control the size of the resultant nanoparticles. Metal nanoparticles are generated by a technique known as "green synthesis," which uses natural components such as plant extracts or microorganisms (Bibi et al., 2019). The process can produce nanoparticles with unique properties and is more environmentally friendly than alternatives. These methods frequently use plant extracts, microorganisms, or other natural resources as reducing and stabilizing agents rather than more typical chemical reagents that may be detrimental to the environment (Bibi et al., 2019; Gomez-Zavaglia et al., 2022; Rizvi et al., 2022). The plant material is typically cooked or ground into an extract, which is then combined with a metal salt precursor to create nanoparticles. Microbial-mediated methods use some microorganisms, (bacteria and fungi), which have the ability to synthesize nanoparticles. It involves the use of microbial culture or extract as reducing and stabilizing agents. Enzymes are biological catalysts that can be used to produce nanoparticles through enzymatic processes. Lipase, cellulase, and amylase enzymes were used to generate nanoparticles (Gomez-Zavaglia et al., 2022). Microwave-assisted techniques, by shortening the reaction time and temperature, microwave irradiation can be utilized to speed up the synthesis of nanoparticles (Mohammadi et al., 2012). Ultrasonic-assisted techniques, by forming microbubbles that aid in the production of nanoparticles, ultrasonic waves can be utilized to speed up the rate of nanoparticle synthesis (Wei et al., 2023).

In the literature green synthesis methods have been used to produce a variety of electrocatalysts for various applications (Bibi et al., 2019; Gomez-Zavaglia et al., 2022). The choice of electrocatalyst produced by green synthesis depends on the specific application and the desired properties of the electrocatalyst (Ali et al., 2017). The most commonly produced electrocatalysts by green synthesis include, metal nanoparticles (e.g., iron, gold, silver, platinum) which are often used as electrocatalysts in fuel cells, sensors, and other electrochemical devices due to their high surface area, excellent electrical conductivity, and high catalytic activity (Wang & Huang, 2016; Wei et al., 2023). Metal oxides (for example, titanium dioxide and iron oxide) are frequently utilized as electrocatalysts in the breakdown of organic contaminants in water and in the creation of hydrogen gas by water splitting. Because of their high electrical conductivity and wide surface area, carbon-based materials (e.g., graphene, carbon nanotubes) are frequently utilized as electrocatalysts in energy storage devices such as batteries and supercapacitors (Parthasarathy et al., 2020). For this purpose, iron and iron oxide nanoparticles have a wide range of applications due to their unique magnetic and catalytic properties. Some of the most common areas where these nanoparticles are used include biomedical applications (magnetic resonance imaging, drug delivery, and hyperthermia treatment of cancer cells); environmental remediation (removing heavy metals and organic pollutants from contaminated water and soil); energy storage and conversion (ie; lithium-ion batteries and solar cells); catalysis; magnetic data storage; etc (Bibi et al., 2019; Parthasarathy et al., 2020; Wei et al., 2023).

Selvaraj et al. (2022) presented the study which is provides an overview of recent developments in the synthesis and application of iron and iron oxide nanoparticles produced by green methods for environmental remediation purposes. They emphasize the benefits of green synthesis

processes, which are more ecologically friendly and sustainable than standard chemical procedures. They discuss the numerous green synthesis strategies used to produce iron and iron oxide nanoparticles, including plant extract-mediated, microorganism-mediated, and green chemistry-based procedures. In addition to their potential applications in environmental remediation, such as the removal of heavy metals, dyes, and other toxins from water and soil, the properties and characteristics of these nanoparticles are explored. In the interest of fully understanding the potential of green synthesized iron and iron oxide nanoparticles for environmental remediation applications and to explore fresh and creative methods to produce these nanoparticles in a sustainable and economical manner, the article emphasizes the need for additional research and development.

Wei et al. (2023) highlighted the difficulty of using water splitting for hydrogen production with electrocatalysts derived from earth-abundant and noble metal-free materials that function effectively throughout a wide pH range. The study reports the development of a spindle-like electrocatalyst made of Co-doped FeP supported on a three-dimensional framework reduced graphene oxide (Co–FeP/3D RGO) using materials such as carbon and iron. The three-dimensional graphene framework supports the growth of FeP and improves its conductivity and stability while the doping of heteroatomic Co enhances the intrinsic activity of FeP. The Co–FeP/3D RGO catalyst demonstrates excellent hydrogen evolution reaction (HER) activity and stability in both acidic and alkaline electrolytes with a lower overpotential and Tafel slope. The study suggests that this research could lead to the development of HER electrocatalysts made of earth-abundant non-precious metals that work well across a wide pH range. In acidic media (0.5 M H_2SO_4), the catalyst exhibited an overpotential of 110.8 mV at a current density of 10 mA/cm^2, and a Tafel slope of 53 mV/decade. In alkaline media (1.0 M KOH), the catalyst exhibited an overpotential of 188 mV at a current density of 10 mA/cm^2, and a Tafel slope of 77.4 mV/decade.

Rizvi et al. (2022) present a green synthesis approach for synthesizing iron oxide nanoparticles by reducing them with pitaya or dragon fruit extract. The benefits of employing pitaya extract as a reducing agent are highlighted in the article, which is a low-cost and ecologically benign alternative to typical chemical reducing agents.

Gomez-Zavaglia et al. (2022) achieved green synthesis, characterization and applications of iron and zinc nanoparticles by probiotics". The purpose of this research is to look into the possibility of using probiotics, specifically lactobacilli and bifidobacteria, for the green synthesis of iron and zinc nanoparticles, as well as to analyze the properties and prospective applications of these nanoparticles. The results revealed that the produced nanoparticles were small in size and had a high degree of crystallinity, making them suitable for a variety of applications. The report also highlighted the possible applications of these nanoparticles in medical, agricultural, and food industries. For example, iron nanoparticles were shown to have antimicrobial capabilities, and zinc nanoparticles were discovered to improve plant growth and agricultural yield.

In this study, iron oxide nanoparticles have been produced using an ethanolic extract of curcuma. It has been selected because the use of herbal extracts in nanoparticle synthesis has several advantages over biological synthesis based on microorganisms, making it an appealing alternative for green nanoparticle synthesis, including several factors such as eco-friendliness, cost-effectiveness, availability, ease of extraction, and reduced risk of contamination.

2. Material and Methods

Fe_2O_3 particles were produced via facile-green synthesis method via curcuma extract without any reducing chemicals. Preparation of curcuma extract was presented below;

A weighed 10 g of curcuma powder was placed in a conical flask (150 mL) contained 100 mL of ethanol (70%). The mixture was shaken well for 5 min, and soaked for two days at room temperature approximately 25-30 ºC. The produced ethanol extract was filtered using qualitative Whatman filter paper no.1 (125 mm) and stored at 4 ºC (Figure 1a). Curcuma (turmeric) is a popular spice in India and many other Asian countries. It included 69.4% carbohydrates, 6.3% protein, 5.1% fat, 3.5% minerals, and 13.1% moisture. Curcumin, in specifically, is a mixture of three curcuminoids [curcumin I ($C_{21}H_2OO_6$, diferuloylmethane, 94%), curcumin II ($C_2OH_{18}O_5$, dimethoxycurcumin, 6%), and curcumin III ($C_{19}H_{16}O_4$, bis-dimethoxycurcumin, 0.3%)] that is known for its yellow color.

Curcumin I ($C_{21}H_2OO_6$, curcumin, diferuloylmethane) is also a significant curcuminoid, as are the phenolic -OH and -CH_2 groups in the -diketone moiety found in turmeric compounds (Vo et al., 2021)

(a) (b)

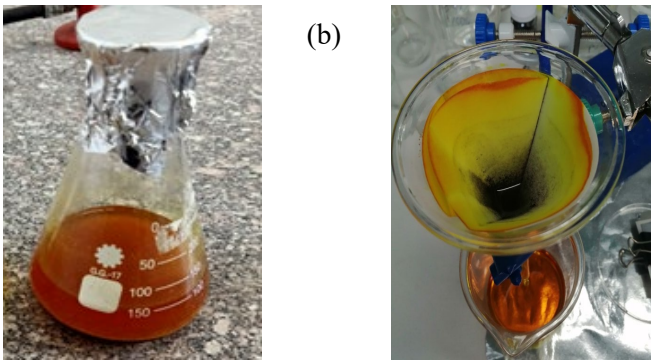

Figure 1. The prepared curcuma ethanol extract (a), after experimental procedure, filtration process of Fe_2O_3 (b).

In the synthesis of Fe_2O_3, iron (III) nitrate solution at the concentration of 10 mM in 50 mL ethanolic extract of curcuma was incubated at 60 °C, for 60 min. This process was achieved in a black room. Afterward, the mixture was cooled at 25 °C for 24 h; subsequently, this mixture was centrifuged 30 min at 3600 rpm. Then, the product acquired was cleaned many times with distilled water and ethanol. Finally, a dark brownish precipitate was shaped, which was desiccated for 1 h at 90 °C (Figure 1b). The reduction of Fe^{3+} is due to the oxidation of the aldehydegroup in curcuma into the carboxylic acid group (Patra & El Kurdi, 2021).

The synthesized Fe_2O_3 particles were monitored via scanning electron microscope (SEM), it was run on JEOL JSM-5500LV. The energy dispersive analysis of EDX for elemental analysis was run using an X-ray micro-analyzer (Oxford 6587, INCA) attached to SEM at 20 kV. Further, Fe_2O_3 particles were analyzed via transmission electron microscope (TEM) samples were run on a (Thermoscientific, Talos F200i) using the carbon-coated grid (Type G 200, 3.05 µ diameter). The zeta potential of Fe_2O_3 particles were achieved via Malvern Panalytical instrument, in the analysis the dispersant was ethanol. The UV-Visible absorption spectroscopy was run on Uni cam UV-VIS spectrophotometer UV2 before and after procedure without washing. The FTIR analysis was done via ATR-FT-IR spectrophotometer (Nicolet iS10 Thermoscientific, serial number AKX1200282). For this purpose solid curcuma, synthesized washed solid Fe_2O_3 and commercial solid Fe_2O_3 samples were investigated.

3. Results and Discussion

The morphological and elemental characterization of synthesized Fe_2O_3 particles were achieved via SEM-EDX analysis and then the deep investigation was done via TEM analysis. While the electron generating and control techniques used by both systems (SEM and TEM) are same, the sample preparation and requirements for TEM are extremely dissimilar (Huang, 2010; Rydz et al., 2019). Thin layers of materials are needed for TEM (often less than 150 nm thick) in order to transmit enough electrons. SEM gives users detailed knowledge of sample surfaces, allowing them to create precise 3D images. In contrast, 2D projections of a sample's interior structure can provided by TEM (Huang, 2010; Rydz et al., 2019). The obtained all electron microscopy results were given Figure 2 and 3, respectively.

Figure 2a showed granular shaped particles with particle sizes ranging between 1.2 and 0.2 µm, which was attributed to agglomeration. As seen in the SEM images, the agglomeration is most likely generated by electrostatic contact between layers of nanoparticle surface. Similar observations have been documented in literature (Mohammadi et al., 2012; Rydz et al., 2019), in order to understand the actual particle size TEM analysis was achieved. According to TEM result in Figure 3, the maximum particle size was almost 80 nm and the minimum particle size was almost 30 nm.

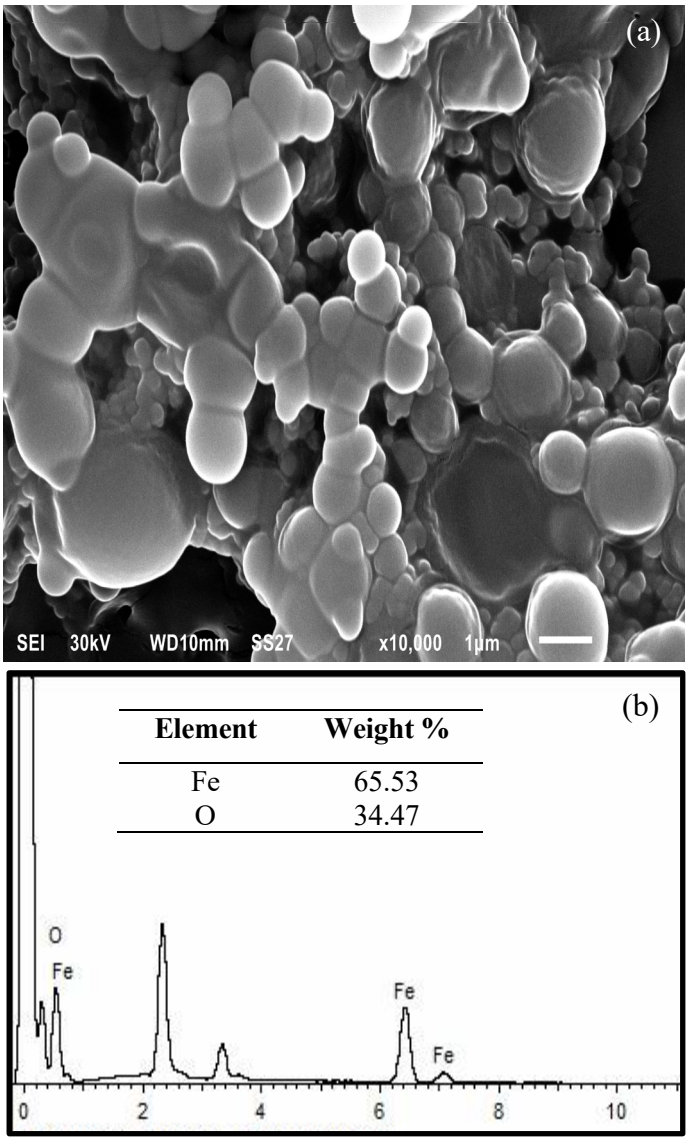

Figure 2. SEM image (a) and EDX results (b) of synthesized Fe_2O_3.

The zeta potential of Fe_2O_3 particles was analyzed and result was presented in Figure 4. The particle and the liquid it is suspended in interact through the zeta potential. It results in attracting and repellent forces between the particles. In a liquid, the same charged particles repel one another whereas different charged particles attract one another. The particle's zeta potential value affects by the attractive and repulsive force (Janusz et al., 1999; Chandransekar et al., 2013). In Figure 4, the obtained value is 11.1 eV. According to the relationship between the zeta potential value and stability of nanoparticles in the literature, particles tend to agglomerate between 0-5 mV (Ateş, 2018). Chandrasekar et al. (2013) declared that the potential exists in the +30 to -30 mV range the particle is said to be stable. According to Meng et al. (2016), the zeta potentials of the iron oxides were varied in the range between 32.5 mV to -19.4 mV. As a consequence, the results of synthesized Fe_2O_3 particles were comparable with literature.

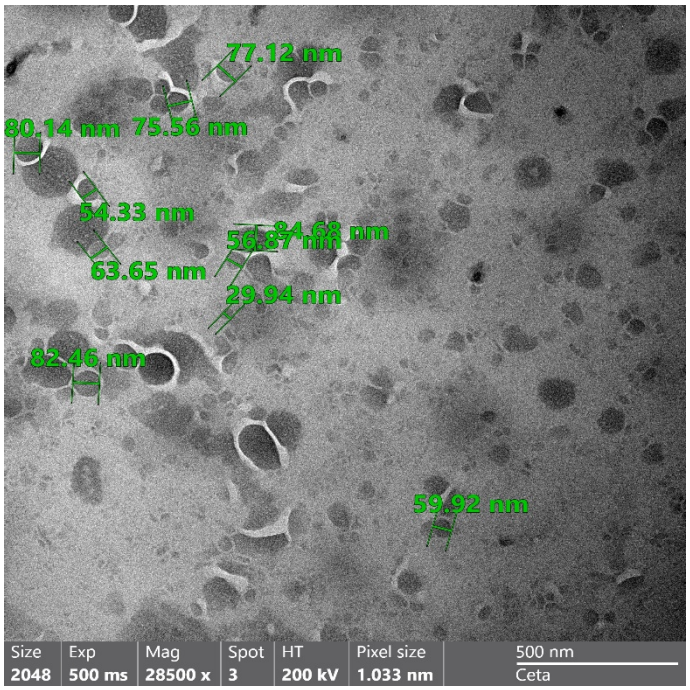

Figure 3. TEM image of synthesized Fe_2O_3.

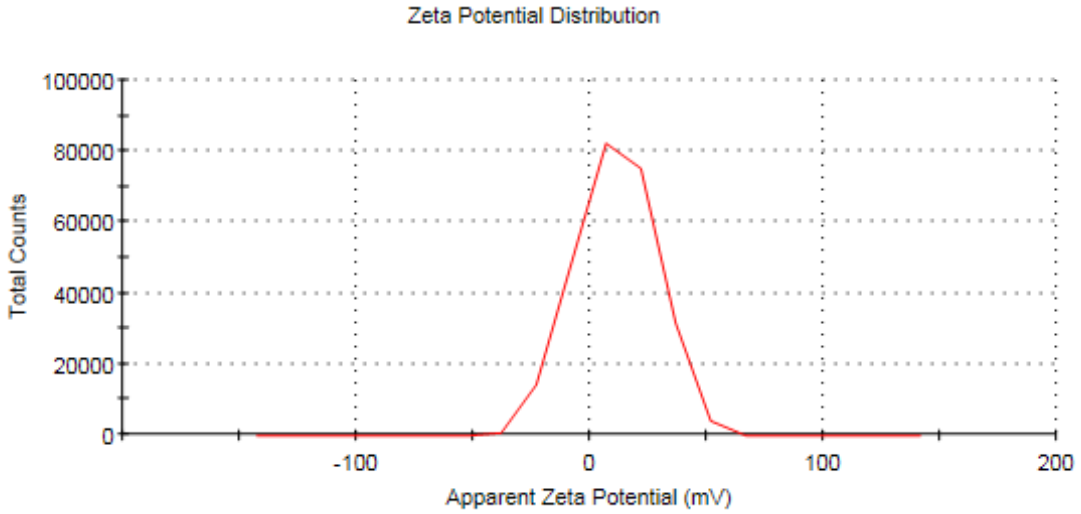

Figure 4. The zetal potential of synthesized Fe_2O_3.

The UV analysis of curcuma extract before (a) and after (b) experimental procedures were achieved and presented in Figure 5.

The interactions of curcuma or a curcumin derivative with Fe^{3+} or Fe^{2+} have been examined spectrophotometrically in the literature (Tcnnesen & Greenhill, 1992). Curcumin and iron ion interactions were seen as an increase in absorbance at 500 nm and a decrease in absorbance at 428 nm. When the concentration of iron ions exceeded that of curcumin, no additional changes in the spectra were seen, confirming the formation of a 1: 1 complex between curcumin and iron ions (Tcnnesen & Greenhill, 1992). In the study of Lassoued et al. (2017), the synthesized Fe_2O_3 with different concentrations of precursor's UV-Vis absorption spectra reveal that all absorption curves display a strong absorption in the 500–700 nm wavelength range. In Figure 5, the peak at 660 nm was associated with synthesized Fe_2O_3 and results were supported with literatüre (Luna et al., 2016; Wang & Huang, 2016; Lassoued et al., 2017; Ali et al., 2017; Parthasarathy et al., 2020).

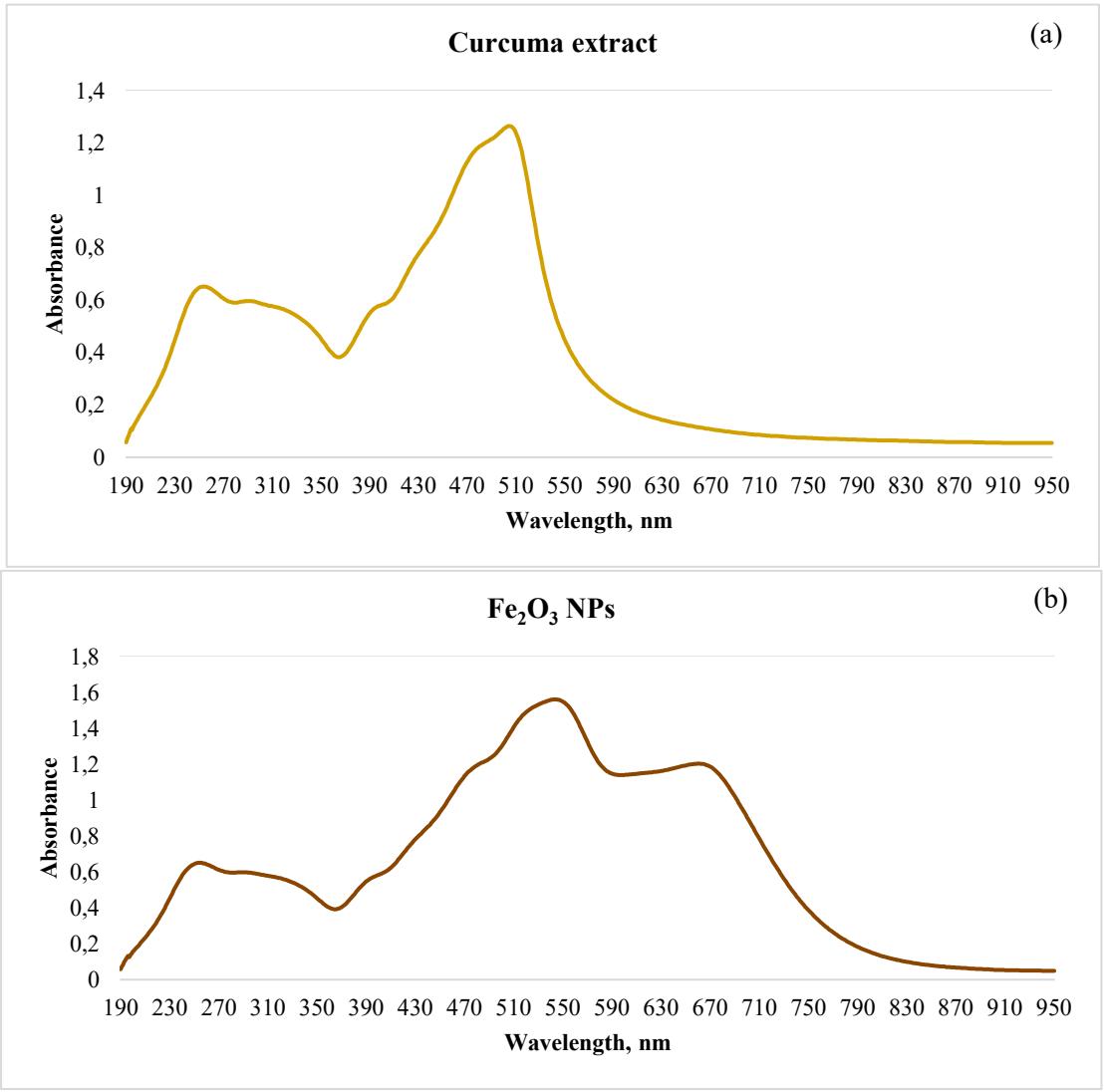

Figure 5. The UV analysis of curcuma extract (a) and synthesized Fe_2O_3 (b).

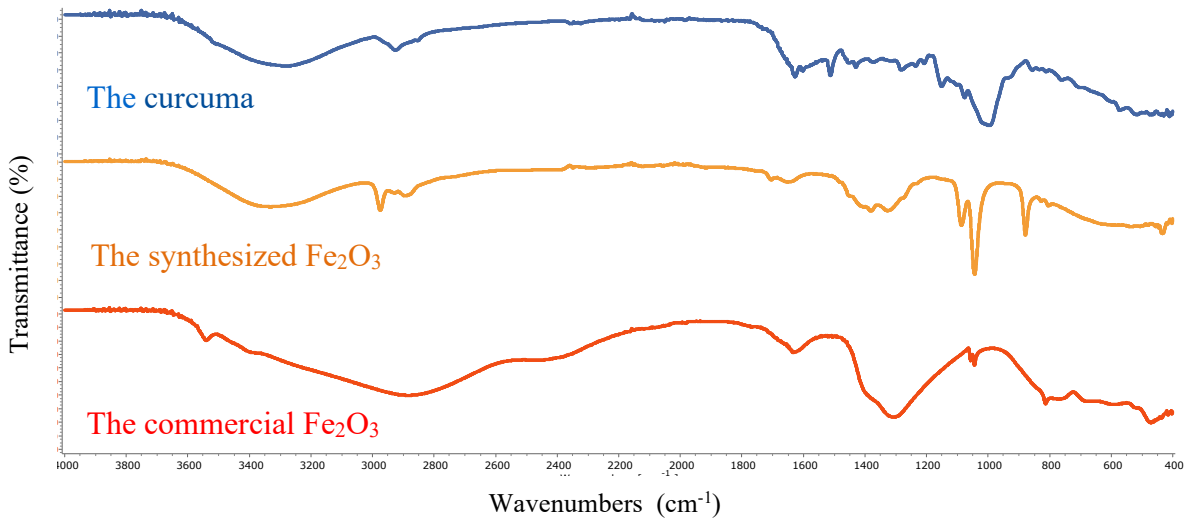

Figure 6. The FTIR aspectra of curcuma extract (a) and synthesized Fe_2O_3 (b).

The structural anaysis of synthesized Fe_2O_3 was achieved via FTIR analysis. The significant bands in the spectra of synthesized Fe_2O_3 (Fig. 6) at 553 cm^{-1}, 605 cm^{-1}, and 878 cm^{-1} can be attributed to Fe-O vibrational modes. The peak at 990 cm^{-1} corresponds to =C–H bond of alkenes. The peaks at 1045 cm^{-1}, 1160 cm^{-1} and 1315 cm^{-1} were assigned to C–O stretching of alcoholic derivatives. The O–H bending vibrational peak was detected at 1633 cm^{-1} (Qin et al., 2011; Rufus & Philip, 2016; Alshamsi & Hussein, 2018).

The absorption bands between 3012 and 3327 cm^{-1} correspond for both stretching modes surface hydroxyl groups (OH) and the water adsorbed at the surface of Fe_2O_3 (Alshamsi & Hussein, 2018). Some metabolite functional groups, including as alcohols, ketones, and carboxylic acids, were found to be involved in the formation of Fe_2O_3 nanoparticles (Patra & El Kurdi, 2021).

4. Conclusion

The green synthesis method was used to produce iron III oxide (Fe_2O_3) nanoparticles in this study. The ethanolic extract of the powder of the widely available and inexpensive curcuma plant was utilized for this purpose. SEM and TEM were used for morphological examination, and EDX was used for elemental composition investigation. The average particle size ranged between 50 and 80 nm, and the configurations were homogeneous and spherical, according to obtained data. The composition was 65.53% “Fe” and 34.47% “O”. The zeta potential was almost 11 eV, as supported by literature. UV and FTIR results proved Fe_2O_3 nanoparticles were successfully synthesized. The findings revealed that various metabolite functional groups were involved in the creation of Fe_2O_3 nanoparticles. It is intended to conduct application investigations of these particles in subsequent studies.

References

Ali, H. R., Nassar H. N., & El-Gendy, N. S. (2017). Green synthesis of α-Fe_2O_3 using Citrus reticulum peels extract and water decontamination from different organic pollutants. *Energy Sources, Part A: Recovery, Utilization, and Environmental Effects*, 39(13), 1425-1434. doi:10.1080/15567036.2017.1336818

Alshamsi, H. A., Hussein, B. S. (2018). Synthesis, characterization and photocatalysis of g-Fe_2O_3 nanoparticles for degradation of cibacron brilliant yellow 3G-P. *Asian Journal of Chemistry*, 30(2), 273-279. doi:10.14233/ajchem.2018.20888

Ateş, M. (2018). Nanoparçacıkların ölçme ve inceleme teknikleri. *Turkish Journal of Scientific Reviews*, 11(1), 63-69.

Bibi, I., Nazar, N., Ata, S., Sultan, M., Ali, A., Abbas, A., … & Iqbal, M. (2019). Green synthesis of iron oxide nanoparticles using pomegranate seeds extract and photocatalytic activity evaluation for the degradation of textile dye. *Journal of Materials Research and Technology*, 8(6), 6115-6124. doi:10.1016/j.jmrt.2019.10.006

Chandransekar, N., Kumar, K. M. M., Balasubramnian, K. S., Karrunamurthy, K., & Varadharajan, R. (2013). Facile synthesis of iron oxide, iron-cobalt and zero valent iron nanoparticles and evaluation of their antimicrobial activity, free radicle scavenginging activity and antioxidant assay. *Digest Journal of Nanomaterials and Biostructures*, 8(2), 765-775.

Gomez-Zavaglia, A., Cassani, L., Hebert, E. M., & Gerbino, E. (2022). Green synthesis, characterization and applications of iron and zinc nanoparticles by probiotics. *Food Research International*, 155, 111097. doi:10.1016/j.foodres.2022.111097

Huang, B. (2010). Super-resolution optical microscopy: multiple choices. *Current Opinion in Chemical Biology*, 14(1), 10-14. doi:10.1016/j.cbpa.2009.10.013

Janusz, W., Sworska, A., & Szczypa, J. (1999). Electrical double layer at the a-Fe_2O_3–mixed electrolyte (ethanol–aqueous) interface. *Colloids and Surfaces A: Physicochemical and Engineering Aspects*, 149(1-3), 421-426. doi:10.1016/S0927-7757(98)00561-5

Lassoued, A., Dkhil, B., Gadri, A., & Ammar, S. (2017). Control of the shape and size of iron oxide (α-Fe_2O_3) nanoparticles synthesized through the chemical precipitation method. *Results in Physics*, 7, 3007-3015. doi:10.1016/j.rinp.2017.07.066

Luna, C., Cuan-Guerra, A. D., Barriga-Castro, E. D., Núñez, N. O., & Mendoza-Reséndez, R. (2016). Confinement and surface effects on the physical properties of rhombohedral-shape hematite (α-Fe_2O_3) nanocrystals. *Materials Research Bulletin*, 80, 44-52. doi:10.1016/j.materresbull.2016.03.029

Meng, X., Ryu, J., Kim, B., & Ko, S. (2016). Application of iron oxide as a pH-dependent indicator for improving the nutritional quality. *Clinical Nutrition Research*, 5(3), 172-179. doi:10.7762/cnr.2016.5.3.172

Mohammadi, S. Z., Khorasani-Motlagh, M., Jahani, S., & Yousefi, M. (2012). Synthesis and characterization of α-Fe_2O_3 nanoparticles by microwave method. *International Journal of Nanoscience and Nanotechnology*, 8(2), 87-92.

Parthasarathy, V., Selvi, J., Senthil Kumar, P., Anbarasan, R., & Mahalakshmi, S. (2020). Evaluation of mechanical, optical and thermal properties of PVA nanocomposites embedded with Fe_2O_3 nanofillers and the investigation of their thermal decomposition characteristics under non-isothermal heating condition. *Polymer Bulletin*, 78(4), 2191-2210. doi:10.1007/s00289-020-03206-3

Patra, D., & El Kurdi, R. (2021). Curcumin as a novel reducing and stabilizing agent for the green synthesis of metallic nanoparticles. *Green Chemistry Letters and Reviews*, 14(3), 474-487. doi:10.1080/17518253.2021.1941306

Qin, W., Yang, C., Yi, R., & Gao, G. (2011). Hydrothermal synthesis and characterization of single-crystalline -Fe_2O_3 nanocubes. *Journal of Nanomaterials*, 2011, 1-5. doi:10.1155/2011/159259

Rizvi, M., Bhatia, T., & Gupta, R. (2022). Green & sustainable synthetic route of obtaining iron oxide nanoparticles using Hylocereus undantus (pitaya or dragon fruit). *Materials Today: Proceedings*, 50, 1100-1106. doi:10.1016/j.matpr.2021.07.469

Rufus, A., N, S., & Philip, D. (2016). Synthesis of biogenic hematite (α-Fe_2O_3) nanoparticles for antibacterial and nanofluid applications. *RSC Advances*, 6(96), 94206-94217. doi:10.1039/C6RA20240C

Rydz, J., Šišková, A., & Andicsová Eckstein, A. (2019). Scanning electron microscopy and atomic force microscopy: Topographic and dynamical surface studies of blends, composites, and hybrid functional materials for sustainable future. *Advances in Materials Science and Engineering*, 2019, 1-16. doi:10.1155/2019/6871785

Sarkar, J., Mollick, M. M., Chattopadhyay, D., & Acharya, K. (2017). An eco-friendly route of gamma-Fe_2O_3 nanoparticles formation and investigation of the mechanical properties of the HPMC-gamma-Fe_2O_3 nanocomposites. *Bioprocess and Biosystems Engineering*, 40(3), 351-359. doi:10.1007/s00449-016-1702-x

Selvaraj, R., Pai, S., Vinayagam, R., Varadavenkatesan, T., Kumar, P. S., Duc, P. A., & Rangasamy, G. (2022). A recent update on green synthesized iron and iron oxide nanoparticles for environmental applications. *Chemosphere*, 308(Pt2), 136331. doi:10.1016/j.chemosphere.2022.136331

Tcnnesen, H. H., & Greenhill, J. V. (1992). Studies on curcumin and curcuminoids. XXII: Curcumin as a reducing agent and as a radical scavenger. *International Journal of Pharmaceutics*, 87, 79-87.

Vo, T. S., Vo, T. T. B. C., Vo, T. T. T. N., & Lai, T. N. H. (2021). Turmeric (Curcuma longa L.): chemical components and their effective clinical applications. *Journal of the Turkish Chemical Society Section A: Chemistry*, 8(3), 883-898. doi:10.18596/jotcsa.913136

Wang, C., & Huang, Z. (2016). Controlled synthesis of α-Fe_2O_3 nanostructures for efficient photocatalysis. *Materials Letters*, 164, 194-197. doi:10.1016/j.matlet.2015.10.152

Wei, S., Xing, P., Tang, Z., Wang, Y., & Dai, L. (2023). Spindle-shaped cobalt-doped iron phosphide anchored on three-dimensional graphene electrocatalysis for hydrogen evolution reactions in both acidic and alkaline media. *Journal of Power Sources*, 555, 232414. doi:10.1016/j.jpowsour.2022.232414